Sphaleron Rate of $N_f = 2 + 1$ QCD

Claudio Bonanno,[1,*] Francesco D'Angelo,[2,†] Massimo D'Elia,[2,‡] Lorenzo Maio,[2,3,§] and Manuel Naviglio[2,‖]
[1]Instituto de Física Teórica UAM-CSIC, c/ Nicolás Cabrera 13-15, Universidad Autónoma de Madrid, Cantoblanco, E-28049 Madrid, Spain
[2]Dipartimento di Fisica dell'Università di Pisa & INFN Sezione di Pisa, Largo Pontecorvo 3, I-56127 Pisa, Italy
[3]Aix Marseille Univ., Université de Toulon, CNRS, CPT, Marseille 13009, France

(Received 25 September 2023; revised 4 December 2023; accepted 11 January 2024; published 2 February 2024)

We compute the sphaleron rate of $N_f = 2 + 1$ QCD at the physical point for a range of temperatures 200 MeV $\lesssim T \lesssim$ 600 MeV. We adopt a strategy recently applied in the quenched case, based on the extraction of the rate via a modified version of the Backus-Gilbert method from finite-lattice-spacing and finite-smoothing-radius Euclidean topological charge density correlators. The physical sphaleron rate is finally computed by performing a continuum limit at fixed physical smoothing radius, followed by a zero-smoothing extrapolation. Dynamical fermions were discretized using the staggered formulation, which is known to yield large lattice artifacts for the topological susceptibility. However, we find them to be rather mild for the sphaleron rate.

DOI: 10.1103/PhysRevLett.132.051903

Introduction.—The rate of real-time QCD topological transitions, the so-called strong sphaleron rate,

$$\Gamma_{\rm sphal} = \lim_{\substack{V_s\to\infty \\ t_{\rm M}\to\infty}} \frac{1}{V_s t_{\rm M}} \left\langle \left[\int_0^{t_{\rm M}} dt'_{\rm M} \int_{V_s} d^3x q(t'_{\rm M}, \vec{x}) \right]^2 \right\rangle = \int dt_{\rm M} d^3x \langle q(t_{\rm M}, \vec{x}) q(0,\vec{0}) \rangle, \quad (1)$$

where $t_{\rm M}$ is the Minkowski time and $q = (\alpha_s/8\pi) G\tilde{G}$ is the QCD topological charge density, plays a crucial role in several phenomenological contexts.

For example, during heavy-ion collisions, where a hot medium of quarks and gluons and strong magnetic fields are created for a short time, a nonvanishing sphaleron rate in the quark-gluon plasma can create local imbalances in the number of left- and right-handed quark species, leading in particular to the so-called chiral magnetic effect [1–5], i.e., the appearance of an electric current flowing in the quark-gluon medium in the parallel direction to the magnetic field.

Another example is offered by axion phenomenology, where recently it has been argued that the strong sphaleron rate plays an intriguing role [6]. As a matter of fact, the QCD strong sphaleron rate describes the rate of axion creation and annihilation in the early Universe, and such quantity directly enters the Boltzmann equation for the time evolution of the axion number distribution in the cosmological medium.

It is therefore clear that a first-principles and fully nonperturbative computation of the QCD sphaleron rate at finite temperature constitutes an essential input to provide fundamental phenomenological predictions about the Standard Model and beyond. However, so far results in the literature have been limited to the quenched case, i.e., the pure-gauge Yang-Mills theory [7–11].

In this Letter we present a first nonperturbative determination of the sphaleron rate in $2 + 1$ QCD at the physical point from numerical Monte Carlo simulations on the lattice above the chiral crossover. In particular, we explored a temperature range 200 MeV $\lesssim T \lesssim$ 600 MeV, and the rate was computed adopting the strategy we recently applied in the quenched case in [11].

Methods.—We performed Monte Carlo simulations of $N_f = 2 + 1$ QCD at the physical point for five temperatures: $T = 230$, 300, 365, 430, and 570 MeV. For each temperature, we explored 3–5 values of the lattice spacing, keeping the physical lattice volume constant and choosing the bare coupling and the bare quark masses so as to move on a line of constant physics, where $m_s/m_l = 28.15$ and $m_\pi \simeq 135$ MeV were kept constant and equal to their physical value [12–14]. The gauge sector has been discretized by using the tree-level Symanzik improved Wilson gauge action, while the quark sector was discretized adopting rooted stout staggered fermions.

Gauge configurations have been generated adopting the standard rational hybrid Monte Carlo updating algorithm, used in combination with the multicanonical algorithm. Above the QCD chiral crossover $T_c \simeq 155$ MeV, the topological susceptibility $\chi \equiv \langle Q^2 \rangle / V$, $Q = \int d^4x\, q(x)$,

is suppressed as a power law of the temperature [15–18]. Because of such suppression, on typical lattice volumes $\langle Q^2 \rangle = V\chi \ll 1$, topological fluctuations are suppressed and the probability distribution of Q is dominated by $Q = 0$. Thus, large statistics are needed to properly sample the topological charge distribution. The multicanonical algorithm allows one to easily bypass this issue by adding a topological bias potential to the gauge action that enhances the probability of visiting suppressed topological sectors, without spoiling importance sampling. Expectation values with respect to the original path-integral probability distribution are then exactly recovered via a standard reweighting [18–21].

The first step to determining the sphaleron rate is to obtain Euclidean lattice topological charge density correlators. The charge density was discretized using the standard gluonic clover definition:

$$q_L(n) = \frac{-1}{2^9\pi^2} \sum_{\mu\nu\rho\sigma=\pm 1}^{\pm 4} \varepsilon_{\mu\nu\rho\sigma} \mathrm{Tr}\{\Pi_{\mu\nu}(n)\Pi_{\rho\sigma}(n)\}, \quad (2)$$

where $\Pi_{\mu\nu}(n)$ is the plaquette and $\varepsilon_{(-\mu)\nu\rho\sigma} = -\varepsilon_{\mu\nu\rho\sigma}$.

We first compute the time profile $Q_L(n_t)$ of the topological charge Q_L:

$$Q_L(n_t) = \sum_{\vec{n}} q_L(n_t, \vec{n}), \qquad Q_L = \sum_n q_L(n). \quad (3)$$

Then, we obtain the topological charge density correlator in dimensionless physical units as

$$\frac{G_L(tT)}{T^5} = \frac{N_t^5}{N_s^3} \langle Q_L(n_{t,1}) Q_L(n_{t,2}) \rangle, \quad (4)$$

where N_s and N_t are the spatial and temporal extents of the lattice and

$$tT = \min\{|n_{t,1} - n_{t,2}|/N_t; 1 - |n_{t,1} - n_{t,2}|/N_t\} \quad (5)$$

is the physical time separation between the sources entering the correlator.

The topological charge profiles are computed on smoothened configurations. Smoothing is used to dampen UV fluctuations affecting the two-point function of the correlator of the lattice topological charge density, which would otherwise result in additive and multiplicative renormalizations [22–25]. Several smoothing algorithms have been proposed, e.g., cooling [26–32], stout smearing [33,34], or gradient flow [35,36], all agreeing when properly matched to each other [32,37,38]. In this work we adopt cooling for its numerical cheapness. A single cooling step consists in aligning each link to its relative staple, so that the local action density is minimized.

Concerning the rate computation, we recall that Eq. (1) is of no use on the lattice, being it expressed in terms of Minkowskian correlators. However, the Kubo equation relates the sphaleron rate to the spectral density $\rho(\omega)$ of the Euclidean topological charge density correlator $G(t) = \int d^3x \langle q(x)q(0) \rangle$ (here t is the imaginary time) [39]:

$$\Gamma_{\mathrm{sphal}} = 2T \lim_{\omega \to 0} \frac{\rho(\omega)}{\omega}, \quad (6)$$

$$G(t) = -\int_0^\infty \frac{d\omega}{\pi} \rho(\omega) \frac{\cosh\{\omega[t - 1/(2T)]\}}{\sinh[\omega/(2T)]}. \quad (7)$$

Therefore, determining the sphaleron rate on the lattice translates into the problem of inverting the integral relation (7) to compute $\rho(\omega)$ from lattice correlators $G_L(t)$. Strategies to solve inverse problems have been widely studied in the literature [9,40–56]. Here we rely on the recently proposed modification [49] of the Backus-Gilbert inversion method [57].

On general grounds, the Backus-Gilbert method assumes that the spectral density can be approximated via

$$\bar{\rho}(\bar{\omega}) = -\pi\bar{\omega} \sum_{t=0}^{1/T} g_t(\bar{\omega}) G(t), \quad (8)$$

where the $g_t(\bar{\omega})$ are unknown coefficients that need to be determined. In our case, we are just interested in $\bar{\omega} = 0$:

$$\left[\frac{\bar{\rho}(\bar{\omega})}{\bar{\omega}}\right]_{\bar{\omega}=0} = -\pi \sum_{t=0}^{1/T} g_t(0) G(t) = \frac{\Gamma_{\mathrm{sphal}}}{2T}. \quad (9)$$

The determination of the g_t coefficients is achieved through the minimization of a suitable functional. In particular we followed the strategy described in Ref. [49], which was also the one we employed in the quenched case in Ref. [11]. Given the technicalities involved in such process, more details on this point are given in the Supplemental Material [58].

The last points to discuss are how to treat finite lattice spacing effects, and what is the impact of smoothing on the sphaleron rate. Let us start recalling that, after n_{cool} cooling steps are performed on the gauge fields, UV fluctuations are damped out, up to a distance known as the smoothing radius $r_s \propto a\sqrt{n_{\mathrm{cool}}}$. The first step, thus, is to take the continuum limit at fixed smoothing radius. In our setup, since $n_{\mathrm{cool}} \propto (r_s/a)^2$ and $N_t^{-1} = aT$, this means to keep $n_{\mathrm{cool}}/N_t^2 \propto (r_s T)^2$ constant for each lattice spacing. Assuming $O(a^2)$ corrections, we perform continuum extrapolations according to the fit function:

$$\Gamma_{\mathrm{sphal},L}\left(N_t, \frac{n_{\mathrm{cool}}}{N_t^2}\right) = \Gamma_{\mathrm{sphal}}\left(\frac{n_{\mathrm{cool}}}{N_t^2}\right) + \frac{c}{N_t^2}, \quad (10)$$

where $\Gamma_{\mathrm{sphal},L}(N_t, n_{\mathrm{cool}})$ stands for the sphaleron rate obtained from the lattice correlator $G_L(tT)$ computed from an $N_s^3 \times N_t$ lattice after n_{cool} cooling steps.

In principle, one would expect a residual dependence of the continuum-extrapolated sphaleron rate on the smoothing radius, i.e., a residual dependence of Γ_{sphal} on n_{cool}/N_t^2. However, for all temperatures we found that Γ_{sphal} is practically independent of n_{cool}/N_t^2 for sufficiently small values of n_{cool}. The same behavior was observed in the quenched theory [11]. Such evidence can be physically explained on the basis of the definition of the rate itself: the dominant contribution to $\rho(\omega)$ in the origin is given by the behavior of the topological charge density correlator at large time separations, and it is reasonable to expect it to be largely unaffected by the UV cutoff introduced by cooling, which mostly affects the short-distance behavior of $G_L(t)$.

Results.—All simulation points are summarized in Table I, while in Table II we summarize our results for the sphaleron rate as a function of the temperature.

First of all, we want to compare our full QCD results with the previous quenched determinations of [7,10,11]. Such comparison is shown in Fig. 1. We observe that full QCD determinations turn out to be slightly larger (although of the same order of magnitude) than the quenched ones, both when we report the rates in terms of the absolute T in MeV, and when we report them in terms of T/T_c, where for full QCD results we used the chiral crossover temperature $T_c = 155$ MeV and for quenched results we used the critical temperature $T_c = 287$ MeV.

We now move to the comparison of our results with available analytical predictions in the literature. In Refs. [59,60], the following semiclassical estimate for the sphaleron rate is reported:

$$\frac{\Gamma_{\mathrm{sphal}}}{T^4} \simeq C_1 \alpha_s^5, \tag{11}$$

with α_s the running strong coupling.

Using the one-loop result for the temperature running of $\alpha_s(T)$ reported in [61], one obtains

$$\frac{\Gamma_{\mathrm{sphal}}}{T^4} = C_1 \left[\frac{C_2}{\log(T^2/\Lambda_{\mathrm{QCD}}^2)}\right]^5 \tag{12}$$

$$\equiv \left[\frac{A_0}{\log(T^2/T_c^2) + \log(B_0^2)}\right]^5, \tag{13}$$

where $B_0 = T_c/\Lambda_{\mathrm{QCD}} \simeq 0.46(2)$ using the latest world-average FLAG value for the 3-flavor dynamically generated scale $\Lambda_{\mathrm{QCD}}^{(\overline{\mathrm{MS}})}(\mu = 2\ \mathrm{GeV}) \simeq 338(12)$ MeV [62], and where the overall prefactor can be estimated to be $A_0 = C_1^{1/5} C_2 \simeq 3.08(2)$ using the expressions for C_1 and C_2 reported, respectively, in Refs. [59,61].

Inspired by the functional form of (12), we performed a best fit of our data for $\Gamma_{\mathrm{sphal}}/T^4$ as a function of T using the following fit function:

$$\frac{\Gamma_{\mathrm{sphal}}}{T^4} = \left[\frac{A}{\log(T^2/T_c^2) + \log(B^2)}\right]^C. \tag{14}$$

Our data are well described by Eq. (14) with $C = 5$, with a reduced chi-squared of 0.36/3. Actually, one should be cautious about this apparent success, in particular regarding the value of C. Indeed, the fit returns a similarly good value of the reduced chi-squared for a very large range of values of C, while if this parameter is left free, the best fit returns a value $C = 5.6$ with a 100% error. This is understandable, since our temperature range is still too small, and our

TABLE I. Summary of simulation parameters. The bare parameters β, am_s and the lattice spacings a have been fixed according to results of Refs. [12–14], and the bare light quark mass am_l is fixed through $m_s/m_l = 28.15$. Simulations marked with * have been performed without multicanonical algorithm as $\langle Q^2 \rangle$ was sufficiently large to observe a reasonable number of fluctuations of the topological charge.

T [MeV]	T/T_c	β	a [fm]	$am_s \times 10^{-2}$	N_s	N_t
230	1.48	3.814*	0.1073	4.27	32	8
		3.918*	0.0857	3.43	40	10
		4.014	0.0715	2.83	48	12
		4.100	0.0613	2.40	56	14
		4.181	0.0536	2.10	64	16
300	1.94	3.938	0.0824	3.30	32	8
		4.059	0.0659	2.60	40	10
		4.165	0.0549	2.15	48	12
		4.263	0.0470	1.86	56	14
365	2.35	4.045	0.0676	2.66	32	8
		4.175	0.0541	2.12	40	10
		4.288	0.0451	1.78	48	12
		4.377	0.0386	1.55	56	14
430	2.77	4.280	0.0458	1.81	32	10
		4.385	0.0381	1.53	36	12
		4.496	0.0327	1.29	48	14
		4.592	0.0286	1.09	48	16
570	3.68	4.316	0.0429	1.71	32	8
		4.459	0.0343	1.37	40	10
		4.592	0.0286	1.09	48	12

TABLE II. Summary of the determinations of the sphaleron rate of $2+1$ full QCD at the physical point.

T [MeV]	$\Gamma_{\mathrm{sphal}}/T^4$
230	0.310(80)
300	0.165(40)
365	0.115(30)
430	0.065(20)
570	0.045(12)

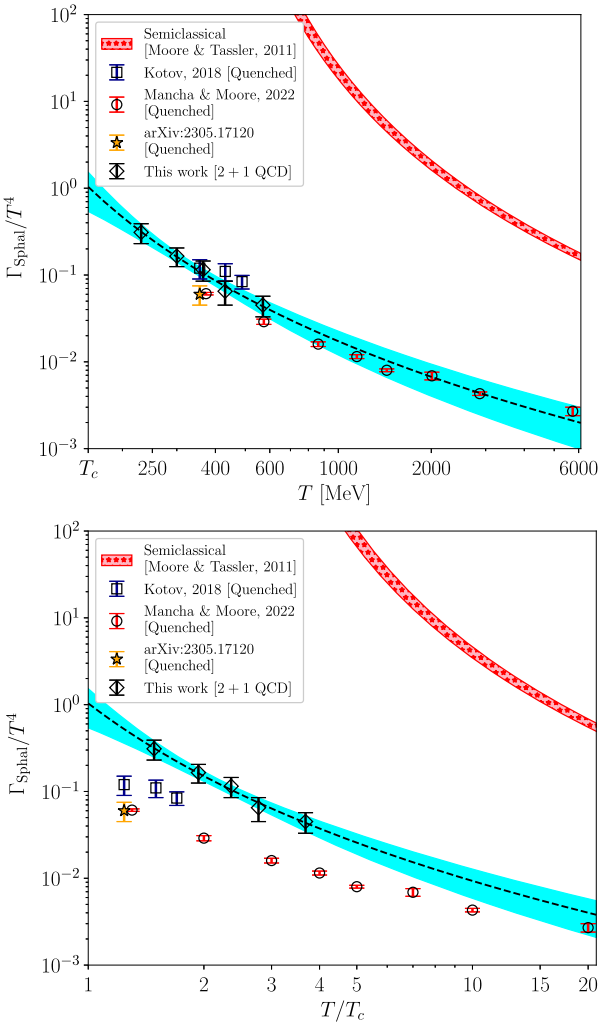

FIG. 1. Sphaleron rate for $2+1$ full QCD at the physical point as a function of temperature T (diamond points). Dashed line and uniform shaded area represent best fit of our results according to (14). Previous quenched determinations of the rate are also shown: Refs. [7,8] (square points), Ref. [10] (round points), and Ref. [11] (starred point). Top plot: x axis expressed in terms of absolute temperature T converted in MeV. Bottom plot: x axis expressed in terms of T/T_c, where $T_c = 155$ MeV and $T_c = 287$ MeV for full QCD and quenched results respectively. Starred shaded area depicts semiclassical prediction (13).

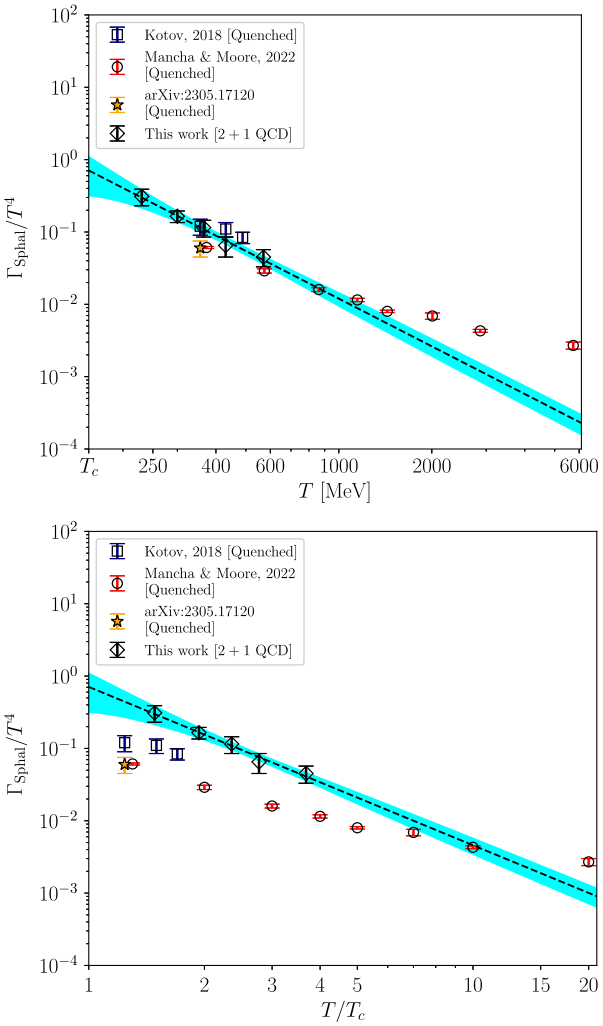

FIG. 2. Same as Fig. 1 but using (15) to fit our data.

statistical errors still too large, to get a precise estimate of the power of a logarithmic function.

If we fix C to the value of the semiclassical prediction, we obtain the best fit depicted in Fig. 1 as a dashed line, while the uniform shaded area represents the corresponding error band; the fit parameters turn out to be $A = 2.96(51)$ and $B = 4.3(1.7)$. We note that we find a remarkable agreement for the prefactor A with the prediction A_0, while we find the pole parameter B to be larger by an order of magnitude compared to B_0. This clarifies why the semiclassical prediction overestimates by more than 2 orders of magnitude the lattice data; cf. Fig. 1.

As a final remark, we would also like to mention that, despite the fact that a semiclassically inspired logarithmic power law fits well our full QCD results for the sphaleron rate, also other functional forms could describe the T behavior of our data. For example, a fit function of the type

$$\frac{\Gamma_{\rm sphal}}{T^4} = \tilde{A}\left(\frac{T}{T_c}\right)^{-b}, \tag{15}$$

works perfectly fine as well, yielding a reduced chi-squared of $0.48/3$, cf. Fig. 2, where the best fit with (15) is depicted as a dashed line and a shaded area. Fit parameters turn out to be $\tilde{A} = 0.71(23)$ and $b = 2.19(38)$.

Conclusions.—In this Letter we presented the first computation of the sphaleron rate in $2+1$ full QCD with physical quark masses as a function of the temperature in the range $200\ \text{MeV} \lesssim T \lesssim 600\ \text{MeV}$.

The sphaleron rate was obtained from the inversion of finite lattice spacing and finite smoothing-radius lattice Euclidean topological charge density correlator from the

modified Backus-Gilbert method recently introduced by the Rome group. Then, the physical value of the sphaleron rate was obtained performing a continuum limit at fixed smoothing radius, followed by a zero-smoothing limit.

Concerning the comparison of our full QCD determinations with previous quenched results, we found them to be larger. Concerning instead the temperature behavior of our data, our results for $\Gamma_{\rm sphal}/T^4$ can be fitted well by a semiclassically inspired functional form, predicting a logarithmic power-law decay of the rate. However, also other functional forms, such as a regular power-law decay of the rate, are shown to describe well our data.

Given that in this work we adopted a nonchiral discretization of the Dirac operator, the recovering of chiral symmetry in the continuum limit is a delicate point. Indeed, it is well known that the explicit breaking of the chiral symmetry of the staggered formulation leads to significant lattice artifacts in the topological susceptibility [15,16,18,20,63–65], that can be mainly traced back to a bad suppression of $Q \neq 0$ charge configurations in the path integral, due to the absence of exact zero modes.

However, as shown in the Supplemental Material [58], thanks to the multicanonic algorithm we can easily compare correlators projected in a fixed topological sector with those obtained without projection. We observe, for our smallest temperature, where χ is less suppressed and thus the weight in the path integral of nonzero charge configurations is larger, that they perfectly agree within errors. This observation points out that a bad suppression of nonzero charge sectors, due to the absence of exact zero modes, cannot be a significant source of lattice artifacts in the sphaleron rate computation. As a matter of fact, we find lattice artifacts for the sphaleron rate to be extremely mild (see Supplemental Material [58]).

Finally, we stress that the same ensembles used here were also employed in [18] to compute the topological susceptibility at finite temperature, and for all temperatures the continuum limit of the gluonic discretization of χ was always confirmed by that obtained from a fermionic discretization based on the lowest-lying modes of the staggered operator [66], which is affected by much smaller artifacts.

In conclusion, these observations make us confident that our continuum extrapolations for $\Gamma_{\rm sphal}$ are reliable. It would be extremely interesting to confirm our findings about the continuum scaling of $\Gamma_{\rm sphal}$ using a different fermionic discretization. Moreover, it would also be extremely interesting to repeat our calculation of the sphaleron rate, employing a different fermionic definition of the lattice topological charge density, based on the index theorem, which is expected to suffer for smaller lattice artifact, or changing the pion mass, to explicitly check the behavior of $\Gamma_{\rm sphal}$ with m_l.

Another intriguing outlook would be to explore higher temperatures towards the GeV scale, in order to better clarify the actual temperature behavior of $\Gamma_{\rm sphal}$. At present, numerical limitations due to the infamous topological freezing problem [67–71] prevent us to reach higher temperatures, which would require one to simulate very fine lattices with $a \lesssim 0.01$ fm, but possible algorithmic developments could permit such simulations in the future [72–76].

Finally, it would be interesting to extend present computations to the case of nonzero spatial momentum $\vec{k}$. As a matter of fact, the momentum dependence of the sphaleron rate is also of great phenomenological interest to compute the axion number density after decoupling using the Boltzmann equation [6].

It is a pleasure to thank G. Gagliardi, V. Lubicz, F. Sanfilippo, G. Villadoro, and J. H. Weber for useful discussions. The work of C. B. is supported by the Spanish Research Agency (Agencia Estatal de Investigación) through the grant IFT Centro de Excelencia Severo Ochoa CEX2020-001007-S and, partially, by grant PID2021-127526NB-I00, both funded by MCIN/AEI. C. B. also acknowledges support from the project H2020-MSCAITN-2018-813942 (EuroPLEx) and the EU Horizon 2020 research and innovation program, STRONG-2020 project, under Grant Agreement No. 824093. Numerical simulations have been performed on the `Marconi` and `Marconi100` machines at CINECA, based on the agreement between INFN and CINECA, under projects INF22_npqcd and INF23_npqcd.

*claudio.bonanno@csic.es
†francesco.dangelo@phd.unipi.it
‡massimo.delia@unipi.it
§lorenzo.maio@phd.unipi.it
‖manuel.naviglio@phd.unipi.it

[1] K. Fukushima, D. E. Kharzeev, and H. J. Warringa, Phys. Rev. D **78**, 074033 (2008).
[2] D. E. Kharzeev, Prog. Part. Nucl. Phys. **75**, 133 (2014).
[3] M. Laine, A. Vuorinen, and Y. Zhu, J. High Energy Phys. 09 (2011) 084.
[4] N. Astrakhantsev, V. V. Braguta, M. D'Elia, A. Y. Kotov, A. A. Nikolaev, and F. Sanfilippo, Phys. Rev. D **102**, 054516 (2020).
[5] G. Almirante, N. Astrakhantsev, V. Braguta, M. D'Elia, L. Maio, M. Naviglio, F. Sanfilippo, and A. Trunin, Proc. Sci. LATTICE2022 (**2023**) 155.
[6] A. Notari, F. Rompineve, and G. Villadoro, Phys. Rev. Lett. **131**, 011004 (2023).
[7] A. Y. Kotov, JETP Lett. **108**, 352 (2018).
[8] A. Y. Kotov, Proc. Sci. Confinement2018 (**2019**) 147.
[9] L. Altenkort, A. M. Eller, O. Kaczmarek, L. Mazur, G. D. Moore, and H.-T. Shu, Phys. Rev. D **103**, 114513 (2021).
[10] M. Barroso Mancha and G. D. Moore, J. High Energy Phys. 01 (2023) 155.
[11] C. Bonanno, F. D'Angelo, M. D'Elia, L. Maio, and M. Naviglio, Phys. Rev. D **108**, 074515 (2023).

[12] Y. Aoki, S. Borsanyi, S. Durr, Z. Fodor, S. D. Katz, S. Krieg, and K. K. Szabo, J. High Energy Phys. 06 (2009) 088.
[13] S. Borsanyi, G. Endrodi, Z. Fodor, A. Jakovac, S. D. Katz, S. Krieg, C. Ratti, and K. K. Szabo, J. High Energy Phys. 11 (2010) 077.
[14] S. Borsanyi, Z. Fodor, C. Hoelbling, S. D. Katz, S. Krieg, and K. K. Szabo, Phys. Lett. B **730**, 99 (2014).
[15] P. Petreczky, H.-P. Schadler, and S. Sharma, Phys. Lett. B **762**, 498 (2016).
[16] S. Borsanyi *et al.*, Nature (London) **539**, 69 (2016).
[17] M. P. Lombardo and A. Trunin, Int. J. Mod. Phys. A **35**, 2030010 (2020).
[18] A. Athenodorou, C. Bonanno, C. Bonati, G. Clemente, F. D'Angelo, M. D'Elia, L. Maio, G. Martinelli, F. Sanfilippo, and A. Todaro, J. High Energy Phys. 10 (2022) 197.
[19] P. T. Jahn, G. D. Moore, and D. Robaina, Phys. Rev. D **98**, 054512 (2018).
[20] C. Bonati, M. D'Elia, G. Martinelli, F. Negro, F. Sanfilippo, and A. Todaro, J. High Energy Phys. 11 (2018) 170.
[21] C. Bonanno, M. D'Elia, and F. Margari, Phys. Rev. D **107**, 014515 (2023).
[22] P. Di Vecchia, K. Fabricius, G. C. Rossi, and G. Veneziano, Nucl. Phys. **B192**, 392 (1981).
[23] M. Campostrini, A. Di Giacomo, and H. Panagopoulos, Phys. Lett. B **212**, 206 (1988).
[24] M. D'Elia, Nucl. Phys. **B661**, 139 (2003).
[25] E. Vicari and H. Panagopoulos, Phys. Rep. **470**, 93 (2009).
[26] B. Berg, Phys. Lett. **104B**, 475 (1981).
[27] Y. Iwasaki and T. Yoshie, Phys. Lett. **131B**, 159 (1983).
[28] S. Itoh, Y. Iwasaki, and T. Yoshie, Phys. Lett. **147B**, 141 (1984).
[29] M. Teper, Phys. Lett. **162B**, 357 (1985).
[30] E.-M. Ilgenfritz, M. Laursen, G. Schierholz, M. Müller-Preussker, and H. Schiller, Nucl. Phys. **B268**, 693 (1986).
[31] M. Campostrini, A. Di Giacomo, H. Panagopoulos, and E. Vicari, Nucl. Phys. **B329**, 683 (1990).
[32] B. Alles, L. Cosmai, M. D'Elia, and A. Papa, Phys. Rev. D **62**, 094507 (2000).
[33] M. Albanese *et al.* (APE Collaboration), Phys. Lett. B **192**, 163 (1987).
[34] C. Morningstar and M. J. Peardon, Phys. Rev. D **69**, 054501 (2004).
[35] M. Lüscher, Commun. Math. Phys. **293**, 899 (2010).
[36] M. Lüscher, J. High Energy Phys. 08 (2010) 071; 03 (2014) 092(E).
[37] C. Bonati and M. D'Elia, Phys. Rev. D **89**, 105005 (2014).
[38] C. Alexandrou, A. Athenodorou, and K. Jansen, Phys. Rev. D **92**, 125014 (2015).
[39] H. B. Meyer, Eur. Phys. J. A **47**, 86 (2011).
[40] D. Boito, M. Golterman, K. Maltman, and S. Peris, Phys. Rev. D **107**, 034512 (2023).
[41] J. Horak, J. M. Pawlowski, J. Rodríguez-Quintero, J. Turnwald, J. M. Urban, N. Wink, and S. Zafeiropoulos, Phys. Rev. D **105**, 036014 (2022).
[42] L. Del Debbio, T. Giani, and M. Wilson, Eur. Phys. J. C **82**, 330 (2022).
[43] A. Candido, L. Del Debbio, T. Giani, and G. Petrillo, Proc. Sci. LATTICE2022 (**2023**) 098.
[44] L. Altenkort, A. M. Eller, O. Kaczmarek, L. Mazur, G. D. Moore, and H.-T. Shu, Phys. Rev. D **103**, 014511 (2021).
[45] L. Altenkort, A. M. Eller, A. Francis, O. Kaczmarek, L. Mazur, G. D. Moore, and H.-T. Shu, Phys. Rev. D **108**, 014503 (2023).
[46] L. Altenkort, O. Kaczmarek, R. Larsen, S. Mukherjee, P. Petreczky, H.-T. Shu, and S. Stendebach (HotQCD Collaboration), Phys. Rev. Lett. **130**, 231902 (2023).
[47] B. B. Brandt, A. Francis, B. Jäger, and H. B. Meyer, Phys. Rev. D **93**, 054510 (2016).
[48] B. B. Brandt, A. Francis, H. B. Meyer, and D. Robaina, Phys. Rev. D **92**, 094510 (2015).
[49] M. Hansen, A. Lupo, and N. Tantalo, Phys. Rev. D **99**, 094508 (2019).
[50] J. Bulava, M. T. Hansen, M. W. Hansen, A. Patella, and N. Tantalo, J. High Energy Phys. 07 (2022) 034.
[51] C. Alexandrou *et al.* (Extended Twisted Mass Collaboration (ETMC)), Phys. Rev. Lett. **130**, 241901 (2023).
[52] R. Frezzotti, N. Tantalo, G. Gagliardi, F. Sanfilippo, S. Simula, and V. Lubicz, Phys. Rev. D **108**, 074510 (2023).
[53] A. Evangelista, R. Frezzotti, G. Gagliardi, V. Lubicz, F. Sanfilippo, S. Simula, and N. Tantalo, Proc. Sci. LATTICE2022 (**2023**) 296.
[54] A. P. Valentine and M. Sambridge, Geophys. J. Int. **220**, 1632 (2019).
[55] A. Rothkopf, EPJ Web Conf. **274**, 01004 (2022).
[56] G. Aarts *et al.*, Prog. Part. Nucl. Phys. **133**, 104070 (2023).
[57] G. Backus and F. Gilbert, Geophys. J. Int. **16**, 169 (1968).
[58] See Supplemental Material at http://link.aps.org/supplemental/10.1103/PhysRevLett.132.051903 for further technical details about the Monte Carlo simulations and the inversion method.
[59] G. D. Moore and M. Tassler, J. High Energy Phys. 02 (2011) 105.
[60] K. V. Berghaus, P. W. Graham, D. E. Kaplan, G. D. Moore, and S. Rajendran, Phys. Rev. D **104**, 083520 (2021).
[61] F. M. Steffens, Braz. J. Phys. **36**, 582 (2006).
[62] Y. Aoki *et al.* (Flavour Lattice Averaging Group (FLAG)), Eur. Phys. J. C **82**, 869 (2022).
[63] C. Bonati, M. D'Elia, M. Mariti, G. Martinelli, M. Mesiti, F. Negro, F. Sanfilippo, and G. Villadoro, J. High Energy Phys. 03 (2016) 155.
[64] J. Frison, R. Kitano, H. Matsufuru, S. Mori, and N. Yamada, J. High Energy Phys. 09 (2016) 021.
[65] C. Alexandrou, A. Athenodorou, K. Cichy, M. Constantinou, D. P. Horkel, K. Jansen, G. Koutsou, and C. Larkin, Phys. Rev. D **97**, 074503 (2018).
[66] C. Bonanno, G. Clemente, M. D'Elia, and F. Sanfilippo, J. High Energy Phys. 10 (2019) 187.
[67] B. Alles, G. Boyd, M. D'Elia, A. Di Giacomo, and E. Vicari, Phys. Lett. B **389**, 107 (1996).
[68] L. Del Debbio, G. M. Manca, and E. Vicari, Phys. Lett. B **594**, 315 (2004).
[69] S. Schaefer, R. Sommer, and F. Virotta (ALPHA Collaboration), Nucl. Phys. **B845**, 93 (2011).

[70] M. Lüscher and S. Schaefer, J. High Energy Phys. 07 (2011) 036.
[71] C. Bonati and M. D'Elia, Phys. Rev. E **98**, 013308 (2018).
[72] M. Hasenbusch, Phys. Rev. D **96**, 054504 (2017).
[73] M. Berni, C. Bonanno, and M. D'Elia, Phys. Rev. D **100**, 114509 (2019).
[74] C. Bonanno, C. Bonati, and M. D'Elia, J. High Energy Phys. 01 (2019) 003.
[75] C. Bonanno, C. Bonati, and M. D'Elia, J. High Energy Phys. 03 (2021) 111.
[76] C. Bonanno, M. D'Elia, B. Lucini, and D. Vadacchino, Phys. Lett. B **833**, 137281 (2022).